# The Possibility of Selective Adsorption and Sensing of the Noble Gaseous Species by the $C_{20}$ Fullerene, the Graphene Sheets, and the $N_4B_4$ Cluster

Parvaneh Pakravan[*]

Department of Chemistry, Zanjan Branch, Islamic Azad University, Zanjan, Iran

## ABSTRACT

There are only a handful reports about the sensor systems having the ability of detecting the existence of the noble gases. Chemical reluctance of these gaseous species causes them to have no chemical interactions like hydrogen bonding with the chemically designed nano-sized sensors. Noble gasses usually have no atomic charges nor do change the total polarity of the molecular sensor systems. These conditions might be more strongly observed for the cases of the lighter noble gases like helium. These properties impede designing molecular sensors for detecting the existence of the noble gasses. Due to these, in this project, we have tried to examine the ability of $N_4B_4$ cluster, $C_{20}$ fullerene, and the graphene segment as especial nano-sized systems in adsorbing and detecting the existence of some noble gasses, by changing their electrical conductivity. The results showed that the $N_4B_4$ cluster could sense the existence of the noble gases, better and more selective than the $C_{20}$ fullerene, or the graphene segment.

**Graphical Abstract**
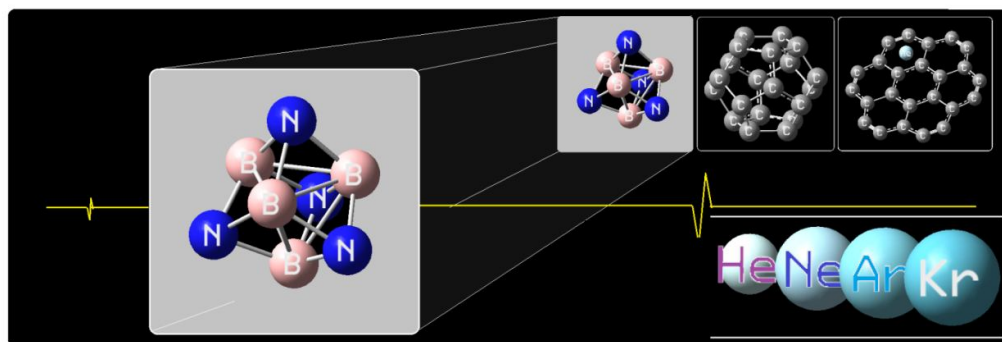
## INTRODUCTION

A gas detector is a device that is able to detect the existence of a gaseous species in an area of a certain space; it could transform a signal to sound an alarm or other forms to operators in the area where a leak occurs [1]. Gas detectors usually have electrochemical [2], infrared point [3], infrared imaging [4], semiconductor

---

[*]Corresponding author: pakravanparvaneh@yahoo.com

[5], ultrasonic [6], or holographic [7] devises; in which, each type is used for proper application. Semiconductor sensors are of the most accurate detectors which transform data from frontier molecular orbital energy changes to electronic signals and even in some cases amplificate those in more clear ones [8]. Also, many researchers from different area of science have focused on semiconducting sensor systems [9,10]. Regarding these, dozens of chemist began to try in developing compositions and especial structures with semiconducting properties for gas sensor applications [11,12]. Along with growth the human knowledge about nano technology, attempts to find nano particles and nano composites with semiconducting properties in order to be used as gas sensors were continued [13]. During a number of precious researches, the possibility of some nano-sized semiconductors containing nanotube CNTs and those derivatives in sensing some of the certain gaseous species, were reported [14,15].

Semiconductor sensors detect gases usually by a physical adsorption or a chemical reaction that takes place when the gas comes in direct contact with the sensor. Metal oxides are the most common materials used in semiconductor sensors [16], and the electrical conductivity of the main mater of the sensor changes when it comes near to the considered gas. The electrical resistance of the semiconductor mater of the sensor is typically around a certain value in kΩ in air; while it changes to another value in kΩ in the presence of the considered gaseous species [17]. This change in resistance is used to calculate the concentration of the gas. Semiconductor sensors are being used in detecting molecular hydrogen, oxygen, alcohol vapor, and hazardous gases such as carbon mono and di-oxide [18].

Between all gaseous species, detection of the noble gasses becomes somewhat more complicated; having no chemical interaction or considerable polar character (especially in the case of the lighter gasses) [19], sense of those species by semiconductor systems is more difficult [20]. Due to this problem, in the present project we have tried to find a new semiconductor matter for sensing the noble gasses, by examining the sensitivity of $N_4B_4$ cluster [21], $C_{20}$ fullerene [17b-d], and the graphene segment [13] to these gases.

## COMPUTATIONAL

Isolated graphene segment and isolated $C_{20}$ fullerene, and $N_4B_4$ cluster, were drawn as input files and were then optimized with each noble gasses to give the best energy minima in every case. During the calculations is it found that for some systems, there was more than one orientation; while, for some other systems, there was only one stable state for each case. The Gaussian 03 quantum chemical package was employed for the required calculations [22] and the considered parameters were extracted accordingly. All stationary states along with the reaction pathways in addition to the other calculation were performed using B3LYP/6-311g (d,p) level of theory [23-25], and the frequencies for each structure were extracted to calculate the thermodynamic and kinetic parameters of each geometry. The natural bond orbital (NBO) analysis [26,27] was subsequently used in order to find the electrical charge of each atom in proposed adsorption sates. The Global Electron Density Transfer (*GEDT*) was calculated using the following formula [28, 29];

$$GEDT = -\Sigma q_A \qquad (1)$$

Where; $q_A$ is the net Mulliken charge as well as the sum covered the entire atoms of dipolarophile species.

The related partial bond order was then extracted using Pauling relation (relation 2) [30];

$$n_X = n_0 \exp \left(\frac{(r_0 - r_x)}{c}\right) \qquad (2)$$

where, the bond order $n_x$ of a bond length $r_x$ is a function of a standard bond of length $r_o$, whose bond order is defined as $n_o$.

## RESULTS
As shown in Figure 1, the isolated graphene segment has a symmetrical structure; while, the complex system congaing the graphene and each of the noble gasses has an asymmetrical geometry. The helium atom of the graphene-He system in Figure 1, is placed in front of the central ring of the graphene, but, it has an asymmetrical distances with the carbon atoms of the graphene ring; somehow, the mentioned distances varies from 4.00 to 4.45 Å. On the other hand, it should be noted that the total distance between helium atom and the graphene sheet is about 3.98 Å. The neon-graphene system has an asymmetrical situation like helium case, somehow the distances between neon atom and the carbon atoms of the central ring of graphene differ from

3.28 to 3.33 Å which has a shorter range compared to the helium-graphene system. As shown in Table 1, the *GEDT* values for the $N_4B_4$ cluster-noble gases systems (0.00, 0.02, 0.00, and 0.04, for He, Ne, Ar, and Kr) are somewhat more than those for the fullerene-noble gases, or graphene segment-noble gases systems (0.00, 0.01, 0.00, and 0.00, for He, Ne, Ar, and Kr), and it shows that the electrical interactions between the $N_4B_4$ cluster and the noble gases is more than the two other considered semiconductors. Also, the average distance between the gases and the sorbent for the $N_4B_4$ cluster (4.02 Å) is lower than those for the fullerene (4.46 Å) or the graphene segment (4.18 Å) which would confirm the stronger interactions between the gas and the sorbent.

In the case of the total distance between the atom and the graphene segment, neon has the lowest distance (2.97 Å) which may show a relatively better adsorption situation. The results of the adsorption parameters presented in Table 1, would confirm this. In the issue of argon and krypton complexes with the graphene sheet, it could be said that those two atoms have the largest total distances with the graphene (4.88 Å for Ar-graphene; and

**Table 1.** The key geometrical distances and the charge densities for the adsorption systems
(X-Y is the distance between the noble gas atom and the sorbent)

| System | X-Y (Å) | *GEDT* | System | X-Y (Å) | *GEDT* |
|---|---|---|---|---|---|
| $C_{20}$ | - | - | Graphene-Ar | 4.88 | 0.00 |
| $C_{20}$-He | 5.29 | 0.00 | Graphene-Kr | 4.89 | 0.00 |
| $C_{20}$-Ne | 3.10 | 0.01 | $N_4B_4$ | - | - |
| $C_{20}$-Ar | 4.45 | 0.00 | $N_4B_4$-He | 4.73 | 0.00 |
| $C_{20}$-Kr | 5.00 | 0.00 | $N_4B_4$-Ne | 3.13 | 0.02 |
| Graphene | - | - | $N_4B_4$-Ar | 5.00 | 0.00 |
| Graphene-He | 3.98 | 0.00 | $N_4B_4$-Kr | 3.23 | 0.04 |
| Graphene-Ne | 2.97 | 0.01 | | | |

4.89 Å for Kr-graphene states), and it may indicate a relatively weaker adsorption interaction between the graphene sheet and each of those two atoms. Also, the symmetrical situations of those these two systems are relatively near to each other; somehow, the distances between the noble atom and the carbon atoms of the graphene central ring varies from 5.04 to 5.14 Å for argon-graphene state, and 5.05 to 5.14 Å for krypton-graphene system.
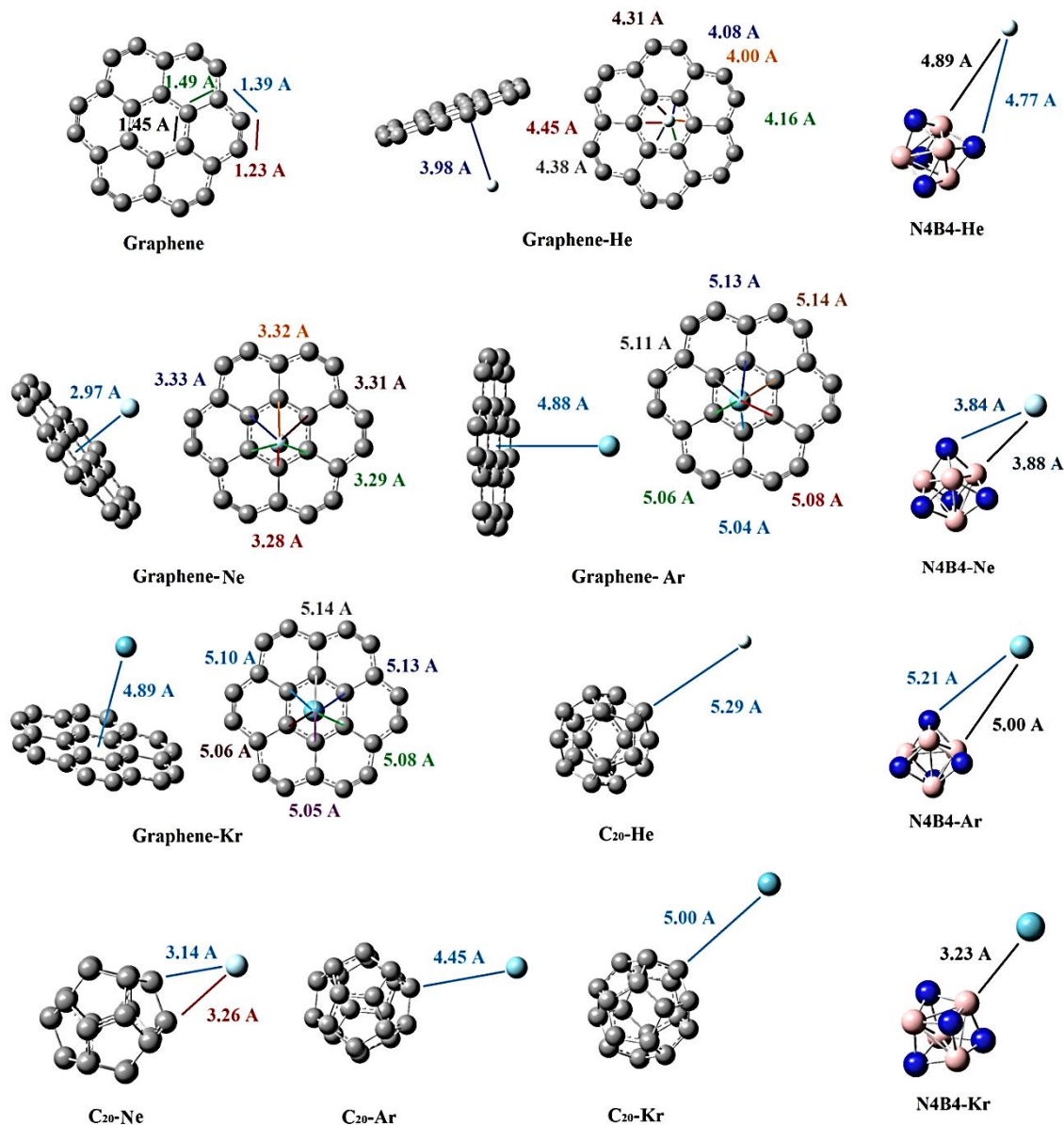
**Fig. 1**. The geometrical situations for the adsorption systems optimized at B3LYP/6-311G(d,p) level of theory.

In the case of adsorption of noble gasses by the $C_{20}$ fullerene, it seems that in each system, at least one symmetrical plane, divides the system in two same parts and it means the asymmetrical situations of the noble atom-graphene systems do not exist in the noble atom fullerene states. As shown in Table 1, the lowest total distance between the noble gas atom and the fullerene belongs to the neon-fullerene system (Figure 1) with an amount of 3.10 Å showing the strongest adsorption state compared to the other parallel systems. The other total distances are 4.45 Å, 5.00 Å, and 5.29 Å which belong to Ar-, Kr-, and He-fullerene systems respectively, which reveal about the relatively weak adsorption interactions. Also, the results of the adsorption and the frontier molecular orbital parameters may prove these.

As given in Table 2, the average value of adsorption energies for the $N_4B_4$ cluster-noble gas systems is -0.422 kcal mol$^{-1}$ (-0.018 kcal mol$^{-1}$, -1.40 kcal mol$^{-1}$, -0.007 kcal mol$^{-1}$, and -0.264 kcal mol$^{-1}$, for He,

Ne, Ar, and Kr, respectively), which is relatively higher than that for graphene (0.214 kcal mol$^{-1}$); and it indicates that the absorption and physical interaction between the noble gas-sorbent system is relatively high for the case of the $N_4B_4$ cluster compared to the graphene segment. The adsorption energies for the fullerene-noble gasses systems show that the strongest adsorption occurs for the neon-fullerene system ($E_{ads}$= -1.14 kcal mol$^{-1}$), and the total distance between neon and the fullerene would confirm this (Figure 1). Also, the *GEDT* value representing the Mulliken charge transfer indicates that the most charge transfer in the case of the fullerene systems occurs for Ne-fullerene state that proves neon atom has the most interaction with the fullerene. After neon, the highest adsorption energies belong to helium- ($E_{ads}$= -0.219 kcal mol$^{-1}$), krypton- ($E_{ads}$= -0.197 kcal mol$^{-1}$), and argon-fullerene ($E_{ads}$= -0.189 kcal mol$^{-1}$) systems which are in agreement with the Mulliken charge transfer values (Table 2).

**Table 2**. The adsorption and frontier molecular orbital FMO parameters of the adsorption systems at B3LYP/6-311G(d,p) level of theory

| System | $E_{ads}$ (kcal mol$^{-1}$) | $E_{HOMO}$ (hartree) | $E_{LUMO}$ (hartree) | $E_g$ (hartree) | $E_g$ (eV) | $\Delta E_g$ (eV) |
|---|---|---|---|---|---|---|
| $C_{20}$ | - | -0.2002 | -0.1289 | -0.0713 | -1.939 | - |
| $C_{20}$-He | -0.219 | -0.2002 | -0.1290 | -0.0711 | -1.936 | -0.0035 |
| $C_{20}$-Ne | -1.14 | -0.1997 | -0.1284 | -0.0713 | -1.939 | 0.0000 |
| $C_{20}$-Ar | -0.189 | -0.2002 | -0.1290 | -0.0711 | -1.936 | -0.0035 |
| $C_{20}$-Kr | -0.197 | -0.2002 | -0.1289 | -0.0712 | -1.938 | -0.0011 |
| Graphene | - | -0.2512 | -0.1222 | -0.1290 | -3.509 | - |
| Graphene-He | -0.003 | -0.2511 | -0.1222 | -0.1289 | -3.508 | -0.0013 |
| Graphene-Ne | -0.819 | -0.2509 | -0.1220 | -0.1289 | -3.507 | -0.0019 |
| Graphene-Ar | -0.006 | -0.2511 | -0.1222 | -0.1289 | -3.508 | -0.0008 |
| Graphene-Kr | -0.031 | -0.1222 | -0.2511 | -0.1289 | -3.507 | -0.0016 |
| $N_4B_4$ | - | -0.3240 | -0.1492 | -0.1748 | -4.737 | - |
| $N_4B_4$-He | -0.018 | -0.3239 | -0.1492 | -0.1748 | -4.736 | 0.0014 |
| $N_4B_4$-Ne | -1.40 | -0.3230 | -0.1479 | -0.1751 | -4.745 | -0.0087 |
| $N_4B_4$-Ar | -0.007 | -0.3243 | -0.1490 | -0.1753 | -4.750 | -0.0054 |
| $N_4B_4$-Kr | -0.264 | -0.3201 | -0.1448 | -0.1752 | -4.748 | 0.0022 |

In the case of the graphene sheet systems, the strongest adsorption occurs for neon atom (like the fullerene systems) which has an adsorption energy value of -0.819 kcal mol$^{-1}$; while krypton (-0.031 kcal mol$^{-1}$), argon- (-0.006 kcal mol$^{-1}$), and helium-graphene (-0.003 kcal mol$^{-1}$) systems have the lowest adsorption energies, respectively. Also, the amounts of charge transfers are in agreement with the order of adsorption energy; somehow the neon-fullerene system with the charge transfer value of +0.010 eV, has the highest value compared to the other noble gas systems. The value of the total distance between neon and graphene sheet (2.97 Å) which is the lowest one (the above mentioned description), compared to the other graphene-gas systems, may confirm the relatively strong interaction in the case of neon-graphene.
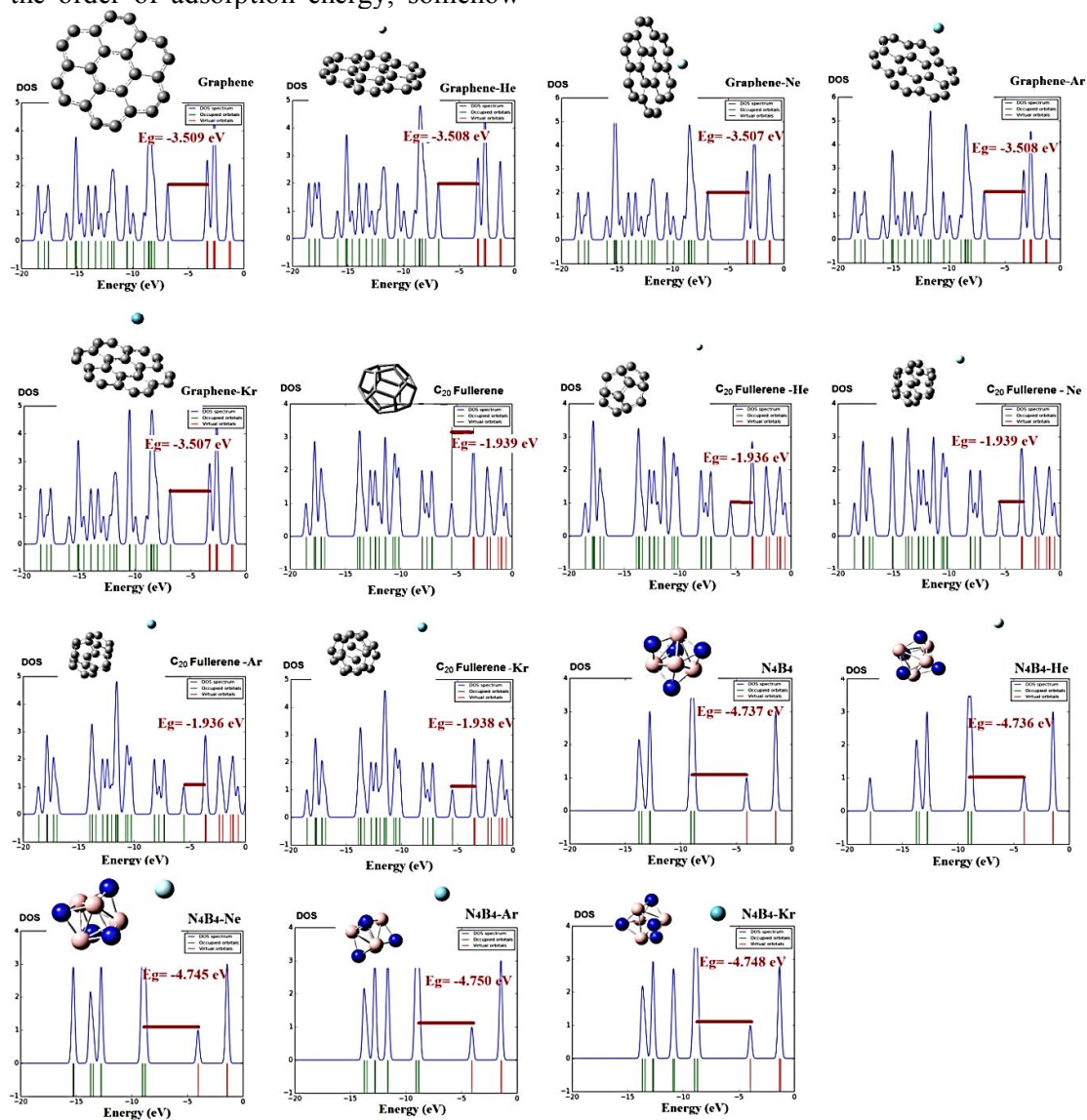


**Fig. 2**. The density of state DOS plots for the adsorption systems of the graphene segments and also for the fullerenes at B3LYP/6-311G(d,p) level of theory.

The results of the DOS plots and the FMO calculations show that presence of helium and argon atoms could change the energy gap of the $C_{20}$ fullerene system from -1.9393 eV (isolated fullerene) to -1.9358 eV that shows the fullerene could sense the presence of those two atoms but not detected those type; while existence of neon atom could not create any change in the fullerene HOMO-LUMO gap (and its electrical conductivity). Also the results show that presence of krypton atom would change the energy gap of the fullerene from -1.9393 eV to -1.9382 eV and it shows that the krypton atom could be sensed by the considered fullerene.

Moreover, the FMO and DOS data shows that presence of each noble gasses species containing helium, neon, argon, and krypton could change the HOMO-LUMO energy gap of the graphene segment from its isolated value (-3.5091) eV, to 3.5078 eV, 3.5083 eV, 3.50875 eV, respectively and it would indicate that each of the noble gasses could be sensed by the considered graphene segment while detecting their types. Also, the results of the DOS spectrums and the FMO analysis show that the changes of the HOMO-LUMO energy gap between the isolated states of the sorbents and the adsorption systems are relatively higher for the case of the $N_4B_4$ cluster; somehow the average of the $/\Delta E_g/$ for the $N_4B_4$-noble gases is 0.0044 eV (0.0014 eV, -0.0087 eV, -0.0054 eV, and 0.002 eV, for He, Ne, Ar, and Kr, respectively) compared to those for the fullerene (0.0020 eV) or for the graphene (0.0014 eV). These show that the sensitivity of the $N_4B_4$ cluster to the noble gases and the potential of this cluster to be a sensor for detecting these gases, are more than the fullerene or the graphene.

## CONCLUSION
The results showed that argon and krypton

complexes with the graphene have the largest total distances with the carbon sheet (4.88 Å for Ar-graphene; and 4.89 Å for Kr-graphene states), and it may reveal about a relatively weaker adsorption interaction between the graphene segment and each of those two atoms. On the other hand, the lowest total distance between the noble gas atom and the fullerene belongs to the neon-fullerene system with an amount of 3.10 Å showing the strongest adsorption state compared to the other parallel systems (for the case of the fullerene). The other total distances are 4.45 Å, 5.00 Å, and 5.29 Å which belong to Ar-, Kr-, and He-fullerene systems respectively, resulting in the relatively weak adsorption interactions.

Also, the results show that the sensitivity of the surface of the energy gap between the HOMO and LUMO, for the normal and the adsorbing systems are relatively higher for the case of the $N_4B_4$ cluster; somehow the average of the $/\Delta E_g/$ for the $N_4B_4$-noble gases is 0.0044 eV (0.0014 eV, -0.0087 eV, -0.0054 eV, and 0.002 eV, for He, Ne, Ar, and Kr, respectively) in comparison with those for the fullerene (0.0020 eV) or for the graphene (0.0014 eV), and it indicates that the sensitivity of the $N_4B_4$ cluster to the noble gases and the potential of this cluster for being a sensor for detection these noble gases, are more than the considered fullerene or graphene segment.

## REFERENCES
[1] G. Keshavaditya, G.R. Eranna, G. Eranna, PRT Embedded Microheaters for Optimum Temperature Distribution of Air-Suspended Structures for Gas Sensor Applications. IEEE Sens. J. 15 (2015) 4137-4140.
[2] M. Liu, S. He, W. Chen, $Co_3O_4$ nanowires supported on 3D N-doped

carbon foam as an electrochemical sensing platform for efficient $H_2O_2$ detection. Nanoscale 6 (2014) 11769-11776.

[3] D.W.T. Griffith, M.M. Deutscher, C. Caldow, G. Kettlewell, M. Riggenbach, S. Hammer, A Fourier transform infrared trace gas and isotope analyser for atmospheric applications. Atmos Meas. Tech. 5 (2012) 2481-2498.

[4] L. Nugent-Glandorf, T. Neely, F. Adler, A.J. Fleisher, K.C. Cossel, B. Bjork, T. Dinneen, J. Ye, S.A. Diddams, Mid-infrared virtually imaged phased array spectrometer for rapid and broadband trace gas detection. Opt. let. 37 (2012) 3285-3287.

[5] S.W. Choi, A. Katoch, J. Zhang, S.S. Kim, Electrospun nanofibers of CuO $SnO_2$ nanocomposite as semiconductor gas sensors for H 2 S detection. Sens. Actuat. B-Chem. 176 (2013) 585-591.

[6] T. Scheller, W. Heinze, J. Schreyer, R. Wysotzky, Ultrasonic sensor for the detection of gas bubbles. U.S. Patent 4,722,224, 1988.

[7] J.L. Martinez-Hurtado, C.A.B. Davidson, J. Blyth, C.R. Lowe, Holographic detection of hydrocarbon gases and other volatile organic compounds. Langmuir 26 (2010) 15694-15699.

[8] J.Y. Fu, D. Wu, B.T. Zhou, Y. Yuan, H.Y. Yan, Design and Analysis of Multilayer Semiconductor Sensor for Acetone Gas Sensing. In. Appl. Mech. Mater. 687 (2014) 1113-1116.

[9] Y.H. Lin, A. Das, MH. Wu, T.M. Pan, C.S. Lai, Microfluidic chip integrated with an electrolyte-insulator-semiconductor sensor for pH and glucose level measurement. Int. J. Electrochem. Sci. 8 (2013) 5886-5901.

[10] N. Yamazoe, K. Suematsu, K. Shimanoe, Gas reception and signal transduction of neat tin oxide semiconductor sensor for response to oxygen. Thin Solid Films 548 (2013) 695-702.

[11] L. Zhang, F. Tian, X. Peng, X. Yin, G. Li, L. Dang, Concentration estimation of formaldehyde using metal oxide semiconductor gas sensor array-based e-noses. Sens. Rev. 34 (2014) 284-290.

[12] N. Yamazoe, K. Shimanoe, Proposal of contact potential promoted oxide semiconductor gas sensor. Sens. Actuat. B-Chem. 187 (2013) 162-167.

[13] A. Shokuhi Rad, S.S. Shabestari, S. Mohseni, S.A. Aghouzi, Study on the adsorption properties of $O_3$, $SO_2$, and $SO_3$ on B-doped graphene using DFT calculations. J. Solid State Chem. 237 (2016) 204-210.

[14] A. Shokuhi Rad, Kh. Ayub, Adsorption of pyrrole on $Al_{12}N_{12}$, $Al_{12}P_{12}$, $B_{12}N_{12}$, and $B_{12}P_{12}$ fullerene-like nano-cages; a first principles study. Vacuum 131 (2016) 135-141.

[15] E.A. Velichko, A.I. Nosich, Refractive-index sensitivities of hybrid surface-plasmon resonances for a core-shell circular silver nanotube sensor, Opt. let. 38 (2013) 978-4981.

[16] H.J. Kim, J.H. Lee, Highly sensitive and selective gas sensors using p-type oxide semiconductors: overview. Sens. Actuat. B-Chem. 192 (2014) 607-627.

[17] a) J.W. Yoon, H.J. Kim, H.M. Jeong, J.H. Lee, Gas sensing characteristics of p-type Cr2O3 and Co3O4 nanofibers depending on inter-particle connectivity. Sens. Actuat B-Chem. 202 (2014) 263-271; b) S.A. Siadati, M.S. Amini-Fazl, E. Babanezhad, The possibility of sensing and inactivating the hazardous air pollutant species via

adsorption and their [2+ 3] cycloaddition reactions with $C_{20}$ fullerene. Sens. Actuat. B-Chem. 237 (2016) 591-596; c) S.A. Siadati, N. Nami, Investigation of the possibility of functionalization of $C_{20}$ fullerene by benzene via Diels–Alder reaction. Physica E: Low-dimen. Sys. Nanostruc. 84 (2016) 55-59; d) S.A. Siadati, E. Vessally, A. Hosseinian, L. Edjlali, Possibility of sensing, adsorbing, and destructing the Tabun-2D-skeletal (Tabun nerve agent) by $C_{20}$ fullerene and its boron and nitrogen doped derivatives. Synth. Met. 220 (2016) 606–611.

[18] A. Aijaz, N. Fujiwara, Q. Xu, From metal–organic framework to nitrogen-decorated nanoporous carbons: high $CO_2$ uptake and efficient catalytic oxygen reduction. J. Am. Chem. Soc. 136 (2014) pp.6790-6793.

[19] I.E. Gracheva, V.A. Moshnikov, S.S. Karpova, E.V. Maraeva, Net-like structured materials for gas sensors. JPCS 291(2011) 012017.

[20] S.J. Park, J. Park, H.Y. Lee, S.E. Moon, K.H. Park, J. Kim, S. Maeng, F. Udrea, W.I. Milne, G.T. Kim, High sensitive $NO_2$ gas sensor with low power consumption using selectively grown ZnO nanorods. J. Nanosci. Nanotechnol. 10 (2010) 3385-3388.

[21] a) V.V. Solov'ev, V.V. Malyshev, A.I. Gab, Physicochemical processes at the dielectric/oxide melt interface and their application in the electrocoating of diamond powders, Theor. Found. Chem. Eng. 38 (2004) 205-213; b) Y.A.O. Hai-bo, P.E.I. Ling, The Theoretical Studies on the $B_4N_4$ Cluster, J. Binzhou Uni. 3 (2008) 012.

[22] M.J. Frisch, G.W. Trucks, H.B. Schlegel, G.E. Scuseria, M.A. Robb, J.R. Cheeseman, V.G. Zakrzewski, J.A. Montgomery, Jr., R.E. Stratmann, J.C. Burant, S. Dapprich, J. M. Millam, A.D. Daniels, K.N. Kudin, M.C. Strain, O. Farkas, J. Tomasi, V.Barone, M. Cossi, R. Cammi, B. Mennucci, C. Pomelli, C. Adamo, S. Clifford, J.Ochterski, G.A. Petersson, P.Y. Ayala, Q. Cui, K. Morokuma, D.K. Malick, A.D.Rabuck, K. Raghavachari, J.B. Foresman, J. Cioslowski, J.V. Ortiz, A.G. Baboul,B.B. Stefanov, G. Liu, A. Liashenko, P. Piskorz, I. Komaromi, R. Gomperts, R.L.Martin, D.J. Fox, T. Keith, M.A. Al-Laham, C.Y. Peng, A. Nanayakkara, C.Gonzalez, M. Challa-combe, P.M.W. Gill, B. Johnson, W. Chen, M.W. Wong, J.L. Andres, C. Gonzalez, M. Head-Gordon, E.S. Replogle, J.A. Pople, Gaussian 03 Inc., Pittsburgh; 2003.

[23] A.D. Becke, Density-functional exchange-energy approximation with correct asymptotic behavior. Phys. Rev. A 38 (1988) 3098-3100.

[24] C. Lee, W. Yang, R.G. Parr, Development of the Colle-Salvetti correlation-energy formula into a functional of the electron density. Phys. Rev. B 971 (1988) 785-789.

[25] V.B. Delchev, M.V. Nenkova, Theoretical modeling of the ground state intramolecular proton transfer in cytosine: DFT level study. Acta Chim. Slov. 55 (2008) 132-137.

[26] A.E. Reed, L.A. Curtiss, F. Weinhold, Inter molecular Interactions from a Natural Bond Orbital, Donor-Acceptor Viewpoint. Chem. Rev. 88 (1988) 899-926.

[27] J.E. Carpenter, F.J. Weinhold, Analysis of the geometry of the hydroxyl methyl radical by the "different hybrids for different spins" natural bond orbital procedure. J. Mol. Struct. (Theochem) 169 (1988) 41-62.

[28] L.R. Domingo, A New C-C Bond Formation Model Based on the Quantum Chemical Topology of

Electron Density. RSC Adv. (2014) 32415-32428.

[29] R. Jasiński, In the searching for zwitterionic intermediates on reaction paths of [3+2] cycloaddition reactions between 2, 2, 4, 4-tetramethyl-3-thiocyclobutanone S-methylide and polymerizable olefins. RSC Adv. (2015) 101045-101048.

[30] L. Pauling, Atomic Radii and Interatomic Distances in Metals. J. Am. Chem. Soc. 69 (1947) 542-545.